

Context-sensitive neocortical neurons transform the effectiveness and efficiency of neural information processing

Ahsan Adeel^{1,2,3*}, Mario Franco², Mohsin Raza², Khubaib Ahmed²

Abstract

There is ample neurobiological evidence that context-sensitive neocortical neurons use their apical inputs as context to amplify the transmission of coherent feedforward (FF) inputs. However, it has not been demonstrated until now how this mechanism can provide useful neural computation. Here we show for the first time that the processing and learning capabilities of this form of neural information processing are well-matched to the abilities of mammalian neocortex. Specifically, we show that a network composed of such local processors restricts the transmission of conflicting information to higher levels and greatly reduces the amount of activity required to process large amounts of heterogeneous real-world data e.g., when processing audio-visual speech, these processors use seen lip movements to selectively amplify FF transmission of the auditory information that those movements generate and vice versa. As this mechanism is shown to be over 1250X more efficient (per FF transmission) than the best available forms of deep neural nets, it offers a step-change in understanding the brain's mysterious energy-saving mechanism and inspires advances in designing enhanced forms of biologically plausible machine learning algorithms.

For more than a century, theories of brain function have seen pyramidal cells as integrate-and-fire ‘point’ neurons that integrate all the incoming synaptic inputs in an identical way to compute a net level of cellular activation [1][2]. Recent neurobiological breakthroughs have revealed that context-sensitive two-point layer 5 pyramidal cells (L5PCs) in the mammalian neocortex use their apical inputs as context to modulate the transmission of coherent FF inputs to their basal dendrites (Figure 1) [3][4][5][6][7][8]. Such modulatory regulation via apical dendrites has been associated with the flexibility and reliability of neocortical dynamics [9][10][11]. For example, a rigorous dynamic

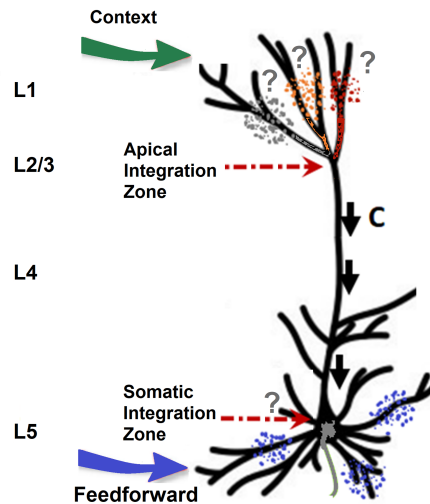


Figure 1: Cooperative context-sensitive neocortical pyramidal cell whose apical dendrites are in layer 1 (L1) with cell body and basal dendrites in deeper layers. The apical tuft receives input from diverse cortical and subcortical sources as context to amplify the transmission of coherent FF signals. However, the information that arrives at the apical tuft, its formation, and the exact nature of its influence on the cell’s response to the FF input remains unclear.

systems perspective [12] suggests that neuromodulation selectively upregulates, and thus flexibly integrates, a subset of disparate cortical regions that would otherwise operate more independently. It is also shown that apical dendrites in layer 1 are the main route by which top-down and other contextual inputs reach L5PCs [13][14][15]. This makes it likely that at least some cells in layers 2 and 3 operate as cooperative context-sensitive neurons because in many regions of many species, these cells have apical dendrites in layer 1 and apical trunks longer than half a millimetre. Furthermore, a recently reported dataset directly recorded from slices of rodent neocortex shows that L5PCs indeed process information in a cooperative context-sensitive manner [16][17][18]. Specifically, the data shows that inputs to the apical dendrites have distinct effects on the output that context sensitivity implies e.g., the L5PC transmits

*¹Oxford Computational Neuroscience Lab, Nuffield Department of Surgical Sciences, University of Oxford, Oxford, UK. ²Conscious Multisensory Integration Lab, University of Wolverhampton, Wolverhampton, UK. ³deepCI.org, Parkside Terrace, Edinburgh, UK. Email: ahsan.adeel@deepci.org

unique information about the FF data without transmitting any unique information about the context. However, depending upon the strength of the FF input, the context adds synergy, which is the information requiring both the context and FF input. These computational studies are the first to test the relationship between context and FF inputs using real rats' somatosensory cortical L5PC data and convincingly validate the biological plausibility of the proposed cooperative context-sensitive style of information processing. In addition, a simulated mouse L5PC model data shows that no action potentials (APs) occur when the FF input is low. APs occur only when: (i) FF input is high, (ii) FF input is low and context input is high, or (iii) both FF and context inputs are high [16][18].

Review evidence also shows unequivocally that changes in brain state such as those from sleeping to waking or from low to high arousal depend on the neuromodulatory regulation of apical function in pyramidal cells [19]. It is shown how impairments of apical dendritic function have a key role in some common neurodevelopmental disorders, including autism spectrum disorders [20]. The apical dendritic mechanisms rooted in genetic foundations experience specific genetic mutations that impair these fundamental cellular mechanisms. A few convincing reviews [21][22][23][24] suggest that the thalamocortical loops with a key role in conscious experience depend on apical dendrites in L1.

Overall, these recent neurobiological reviews and computational models show that the cooperative context-sensitive style of information processing may be fundamental to the abilities of the mammalian neocortex. However, the kinds of information that arrive at the apical tuft and the nature of their influence on the cell's response to the FF input remain unclear. Therefore, it has not been demonstrated until now how this mechanism can provide useful neural computation. Here we address these issues and demonstrate for the first time that the capabilities of this form of neural information processing are well-matched to the capabilities of the mammalian neocortex.

Results

To investigate whether the cooperative context-sensitive style of neural information processing possesses information processing capabilities of the kind displayed by the neocortex, a new biologically plausible multisensory cooperative computing (MCC) architecture is developed (Figure 2). In MCC, neurons use local and universal contextual inputs to dynamically cooperate with other neurons and transmit their FF message only when it is coherently related to the overall activity of the network [25]. This is equivalent to the combined interaction of local and universal contexts with the receptive field (RF) to conditionally segregate the relevant and irrelevant feedforward signals [22][26][27][28]. Here the local context (LC) is fur-

ther divided into local proximal context (C_p) and local distal context (C_d): C_p defines the modulatory signal coming from the neighbouring cell of the same network or the cell's output at time $t-1$, C_d defines the modulatory sensory signal coming from some other parts of the brain (in principle from anywhere in space-time), and universal context (UC), represented as C_u , defines the outside environment and anticipated behavior or widely distributed general context (based on past learning and reasoning) [25]. For simplicity, C_u is linked to brief memory formation and retrieval which is universal in that its modulatory effect is broadcasted to all sensory modalities [29][30]. Figure 2b provides a more detailed flow of information.

The proposed conditional segregation and recombination mechanism aligns with the recent neurobiological studies [22][26][27][28] suggesting that the apical tuft incorporates input from both thalamic and different cortical sources to enable conditional segregation and recombination of multiple input streams. In Figure 2c we show how individual L5PCs can extract synergistic RF components (brief memory) by conditionally segregating the coherent and incoherent multisensory information streams and then recombining only the coherent multistream at time $t-1$. The extracted brief memory components are broadcasted to other brain areas which are received by relevant L5PCs at time t along with the current local context.

The formation of brief memory resonates well with the recent neurobiological study [31][32], suggesting that working memory depends on recurrent amplification combined with divisive normalization. It is shown that such functional models can simulate key sequential phenomena of working memory and motor control. It is also shown how in addition to being temporarily stored, information can be modified by the complex sequential dynamics. Here the brief working memory of the neuron could be seen as if the selected relevant RF is temporarily preserved at time $t-1$, while attention at time t is engaged with the upcoming RF e.g., holding a person's address in mind while listening to instructions about how to get there. This is the ability of the neuron to retain information for a short period of time [14]. Figure 2d hypothesises that the neuron at time $t-1$ is in an unconscious state when the RF e.g., R_{t-1}^a is unmodulated. It moves to a minimally conscious state or content of conscious state when the RF is modulated with LC or both LC and UC, respectively, if they are strong enough [33][34]. The integrated context (C) is constructed as a kernel using a simple adder and a non-linear activation function applied to the processed RF and then fed into the asynchronous modulatory transfer function (AMTF) as explained below.

In previous contextual modulation works [17], it is typically assumed that the firing of two-compartment L5PC is mainly driven by the RF input. If the RF is strong, context is neither necessary nor sufficient for the neuron to transmit informa-

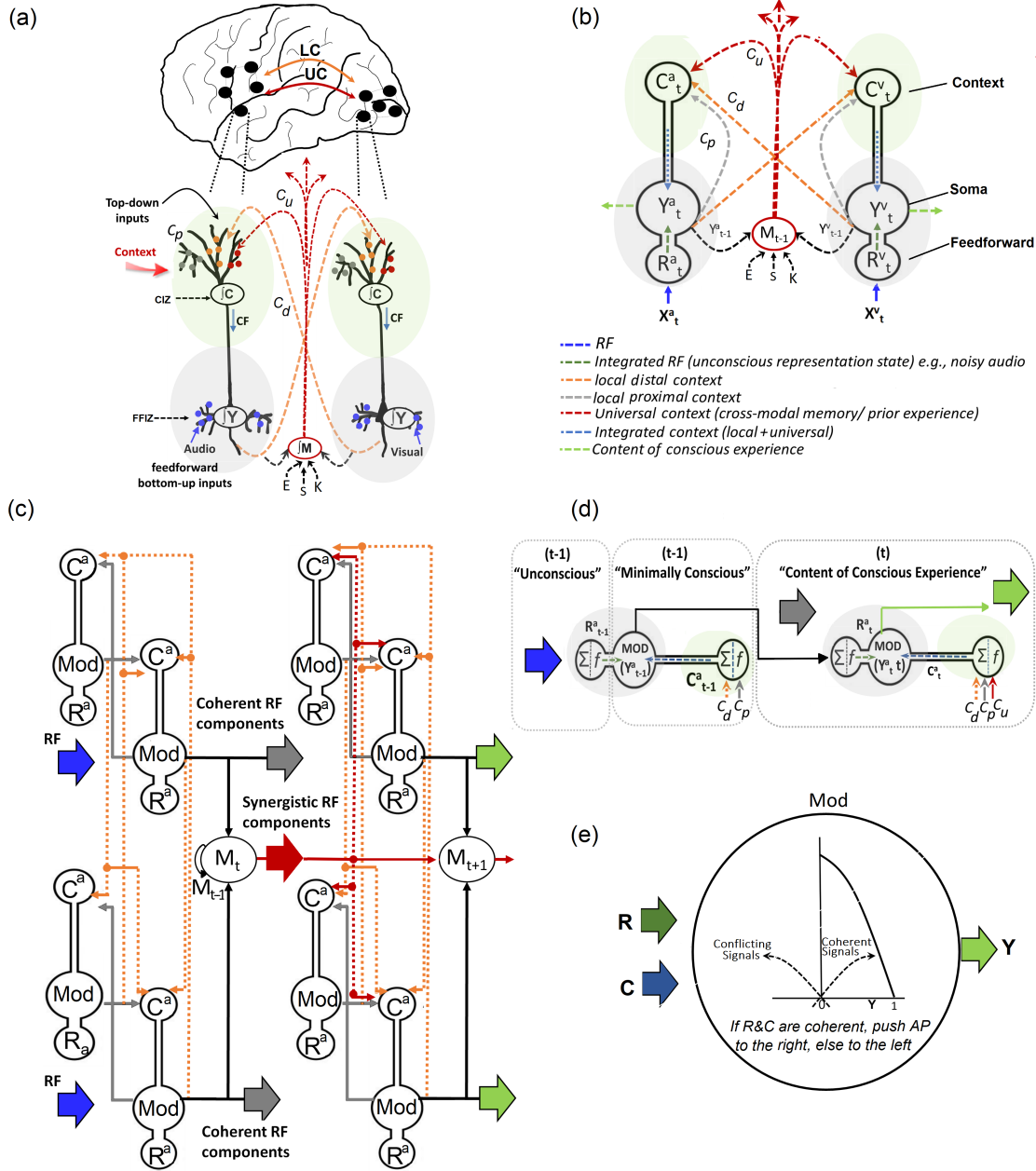


Figure 2: Schematic of biologically plausible cooperative context-sensitive neural information processing and the corresponding multisensory cooperative computing formulation: (a) two-compartment two-unit circuit. The receptive field (RF) in blue arrives at the FF integration zone (FFIZ). The local context (distal in orange and proximal in grey) and the universal context in maroon arrive via synapses at the contextual integration zone (CIZ). RF represents the sensory signal (e.g., noisy audio), local proximal context (C_p) represents the noisy audio coming from the neighbouring cell of the same network or the prior output of the same cell, local distal context (C_p) represents signals coming from other parts of the current external input (e.g., visuals), and the universal context (C_u) represents the brief memory broadcasted to other brain regions. C_u could explicitly be extended to the sources of inputs to include general information about the target domain acquired from prior experiences (E), emotional states (S), and semantic knowledge (K), (b) two-neuron circuit with a detailed flow of information, (c) two-layered computing architecture: neurons in one stream are connected to all other neurons in the same network and the adjacent streams of the second network. Individual neurons cooperate moment-by-moment via local and universal forms of context to separate coherent from conflicting signals, (d) hypothetical neuronal states in scare quotes, and (e) asynchronous modulatory transfer function at the soma that splits the coherent from conflicting signals with the conditional probability of Y : $Pr(Y = 1|R = r, C = c) = p(T(r, c))$, where p is the half-Gaussian filter and $T(r, c)$ is a continuous \mathbb{R}^2 function.

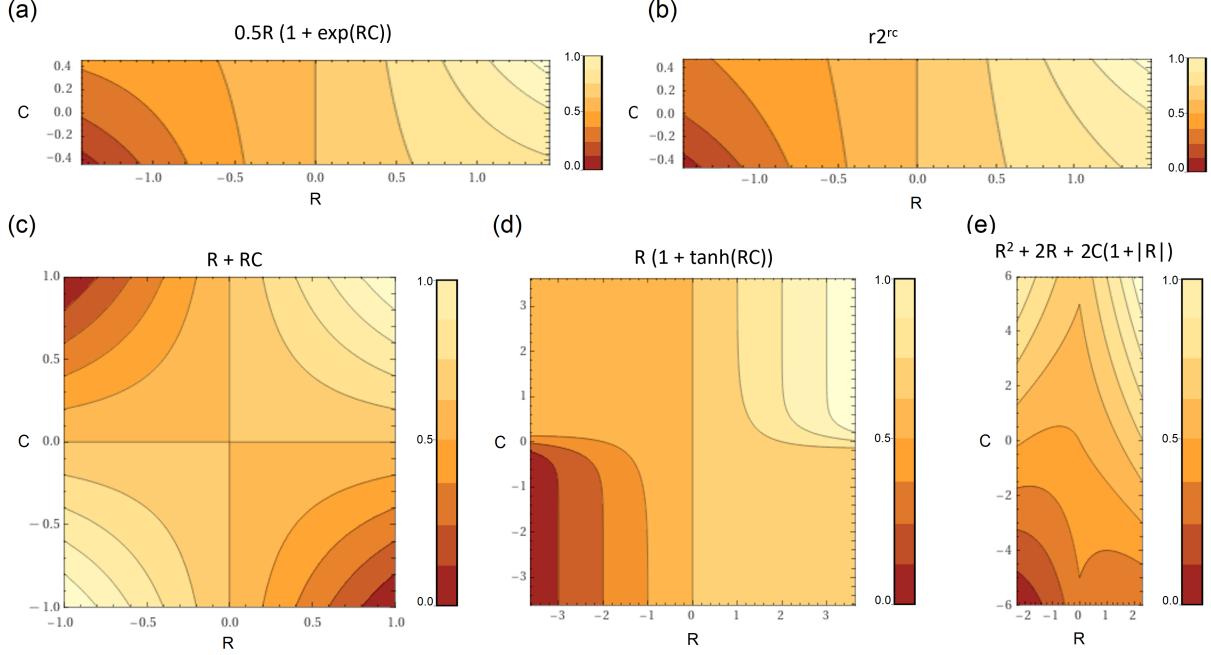


Figure 3: Conventional AMTFs suggest that context modulates the input strength with which they transmit information about other inputs [17] e.g., in a, b, and e, RF (R) is a driving force: when R is very weak, the cell’s AP is zero, and when it is strong, the AP is high regardless of C , whereas (c) is simply an XNOR gate that gives a max output when R and C are same and minimum otherwise. In proposed AMTF (e), C is a driving force that overrules the typical dominance of R and the neural firing is more dependent on the strength of C .

tion about the RF. If the RF is very weak (or does not exist), even a very strong context does not encourage firing. Here we argue that context could overrule the strength of the RF and can conversely discourage or encourage firing if the RF is strong or weak, respectively. For example, the AP in Figure 3(a-c) [17] is high when RF (R) is strong and low when R is weak. However, the AP in Figure 3d strengthens the transmission of information about R when R is weak but never crosses 0.5 threshold even when the context is very strong. In contrast, the proposed AMTF in Figure 3e, discourages or encourages firing if the RF is strong or weak, respectively. This new AMTF uses context as a ‘modulatory force’ to push the action potential (Y) to the right side of the half-Gaussian filter (HGF) if R is important, otherwise to the left as shown in Figure 2e [35]. Nonetheless, the modulatory force that enables this move systematically could be generated in several different ways, linearly or non-linearly e.g., instead of HGF, ReLU with threshold 1 could be used. The modulatory transfer function could be seen as a signalling module that signals ‘Yes’ with certain confidence if a match between data streams has been found regarding a specific sensory or cognitive feature.

Figure 4 depicts the MCC neural model. For the sake of mathematical simplicity and generality across this section, we use Einstein tensor notation. We also reduce the discussion to vector spaces indexed by a single element as in ma-

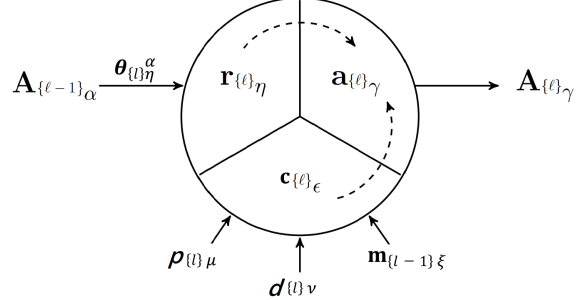


Figure 4: MCC neural model

chine learning we are only interested in numerable collections of vector spaces. Nonetheless, in some cases, it may be useful to include certain topological properties as different indices i.e. an image can be represented as $Z_{\alpha\beta\gamma}$. In addition, we restrict ourselves to the simple case of two channels and denote the analogue variable for the other channel with a bar and, in a huge abuse of notation, we denote every learnable variable with θ . Unlike previous works, our idea is to compute only the relevant information shared between channels while, at the same time, preventing local non-important information from each channel to overtake the computation. Thus, we consider a family \mathcal{F} of parametric functions f composed almost entirely by transformations $h : V_\alpha \times V_{\bar{\alpha}} \mapsto V_\gamma$ which we can express with the

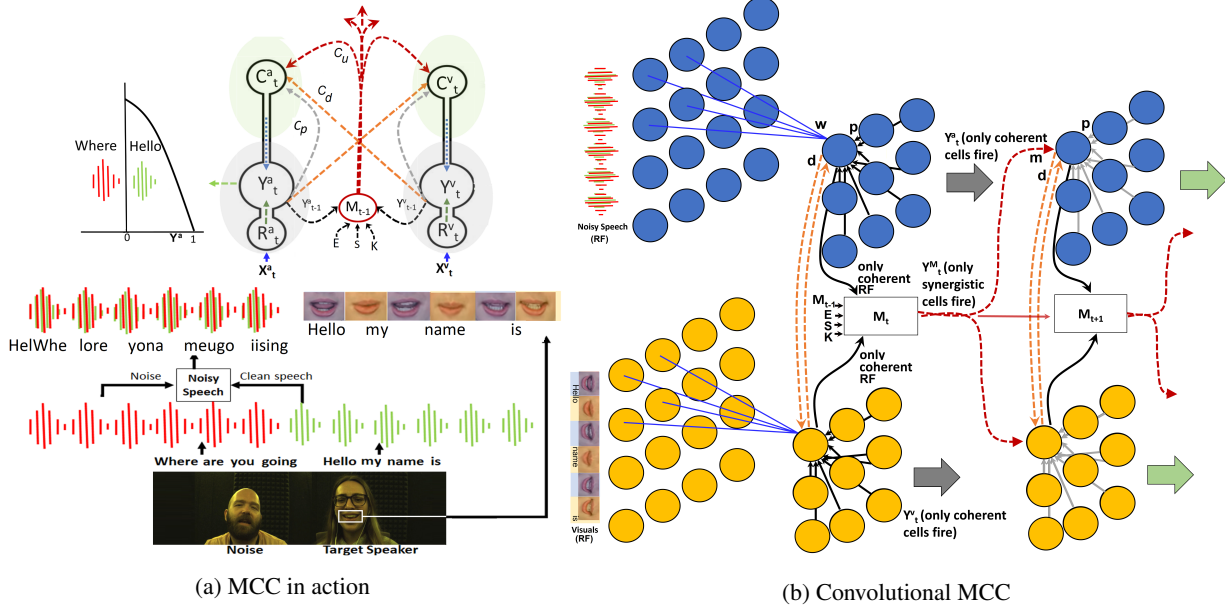


Figure 5: (a) MCC in action: Two persons are talking simultaneously but MCC is cleaning the speech of the speaker whose visuals are available. The processor use seen lip movements to selectively amplify FF transmission of the auditory information that those movements generate and vice versa (b) Convolutional MCC: The neuron in one stream is connected to all other neurons in the adjacent streams of the same layer to effectively coordinate widely distributed and shared activity patterns.

following set of equations,

$$RF : \mathbf{r}_{\{\ell\}\eta} = \theta_{\{\ell\}\eta}^\alpha \mathbf{A}_{\{\ell-1\}\alpha} \quad (1)$$

$$C_p : \mathbf{p}_{\{\ell\}\mu} = \theta_{\{\ell\}\mu}^\eta \mathbf{r}_{\{\ell\}\eta} \quad (2)$$

$$C_d : \mathbf{d}_{\{\ell\}\nu} = \theta_{\{\ell\}\nu}^\tau \bar{\mathbf{r}}_{\{\ell-1\}\tau} \quad (3)$$

$$C_u : \mathbf{m}_{\{\ell-1\}\xi} = \theta_{\{\ell\}\xi}^\rho \mathbf{m}_{\{\ell-2\}\rho} + \theta_{\{\ell\}\xi}^\alpha \mathbf{A}_{\{\ell-1\}\alpha} + \theta_{\{\ell\}\xi}^\beta \bar{\mathbf{A}}_{\{\ell-1\}\beta} \quad (4)$$

$$IC : \mathbf{c}_{\{\ell\}\epsilon} = \theta_{\{\ell\}\epsilon}^{\mu\nu\xi} \mathbf{p}_{\{\ell\}\mu} \mathbf{d}_{\{\ell\}\nu} \mathbf{m}_{\{\ell-1\}\xi} \quad (5)$$

$$\mathbf{a}_{\{\ell\}\gamma} = \Delta_{\gamma}^{\eta\epsilon} \mathbf{r}_{\{\ell\}\eta} \mathbf{c}_{\{\ell\}\epsilon} \quad (6)$$

$$h(\mathbf{A}_{\{\ell-1\}\alpha}, \bar{\mathbf{A}}_{\{\ell-1\}\beta}; \Theta) := \mathbf{A}_{\{\ell\}\gamma} = \zeta(\mathbf{a}_{\{\ell\}\gamma}) \quad (7)$$

where $\Theta = \{\theta_{\{\ell\}\eta}^\alpha, \theta_{\{\ell\}\mu}^\eta, \theta_{\{\ell\}\nu}^\tau, \theta_{\{\ell\}\nu}^\rho, \theta_{\{\ell\}\xi}^\alpha, \theta_{\{\ell\}\xi}^\beta, \theta_{\{\ell\}\epsilon}^{\mu\nu\xi}\}$ is the collection of learnable parametric linear transformations of h ; the operator $\Delta_{\gamma}^{\eta\epsilon}$ denotes the hadamard product between $\mathbf{r}_{\{\ell\}\eta}$ and $\mathbf{c}_{\{\ell\}\epsilon}$. Notice that this implicitly assumes that the vector space of both operands is of the same size, and ζ is the activation function. In practice, we also consider another set of trainable variables $\lambda_{\{\ell\}\kappa}$

which are added to the result of each transformation but including them in the previous equations may obscure the most relevant part of the computation. We can replace the operator $\Delta_{\gamma}^{\eta\epsilon}$ with other operators to simulate a more complex relationship between \mathbf{R} and \mathbf{C} . We suspect that the exploration of better modulatory operators may play a major role in the near future. Intuitively, we enforce variables $\mathbf{p}_{\{\ell\}\nu}$ and $\mathbf{d}_{\{\ell\}\mu}$ to extract the core information that is currently held in the other parallel streams. Similarly, we enforce the term $\mathbf{m}_{\{\ell\}\xi}$ to act as a collective reservoir of important information extracted at a previous layer from both channels.

Simulations: To investigate whether MCC can amplify and suppress the transmission of relevant and irrelevant signals, we started with a representative MCC model optimised for AV speech processing. Figure 5 depicts the MCC-driven AV speech processing model that can reconstruct a clean short-time Fourier transform (STFT) of the audio signal given noisy audio and visuals [36][37]. MCC is compared against three popular DNN approaches: autoencoder (AE), β -variational AE (VAE), and a vanilla version (baseline) of our model (i.e. with standard C3/attention block). For a fair comparison, benchmark state-of-the-art convolutional deep models integrated with the cross-channel communication (C3)/attention blocks are used [38][39][40][41]. These models implement C3 or cross-channel fusion through concatenation, addition, or multiplication using the ‘point’ neuron model [2]. Thus, each neuron integrates

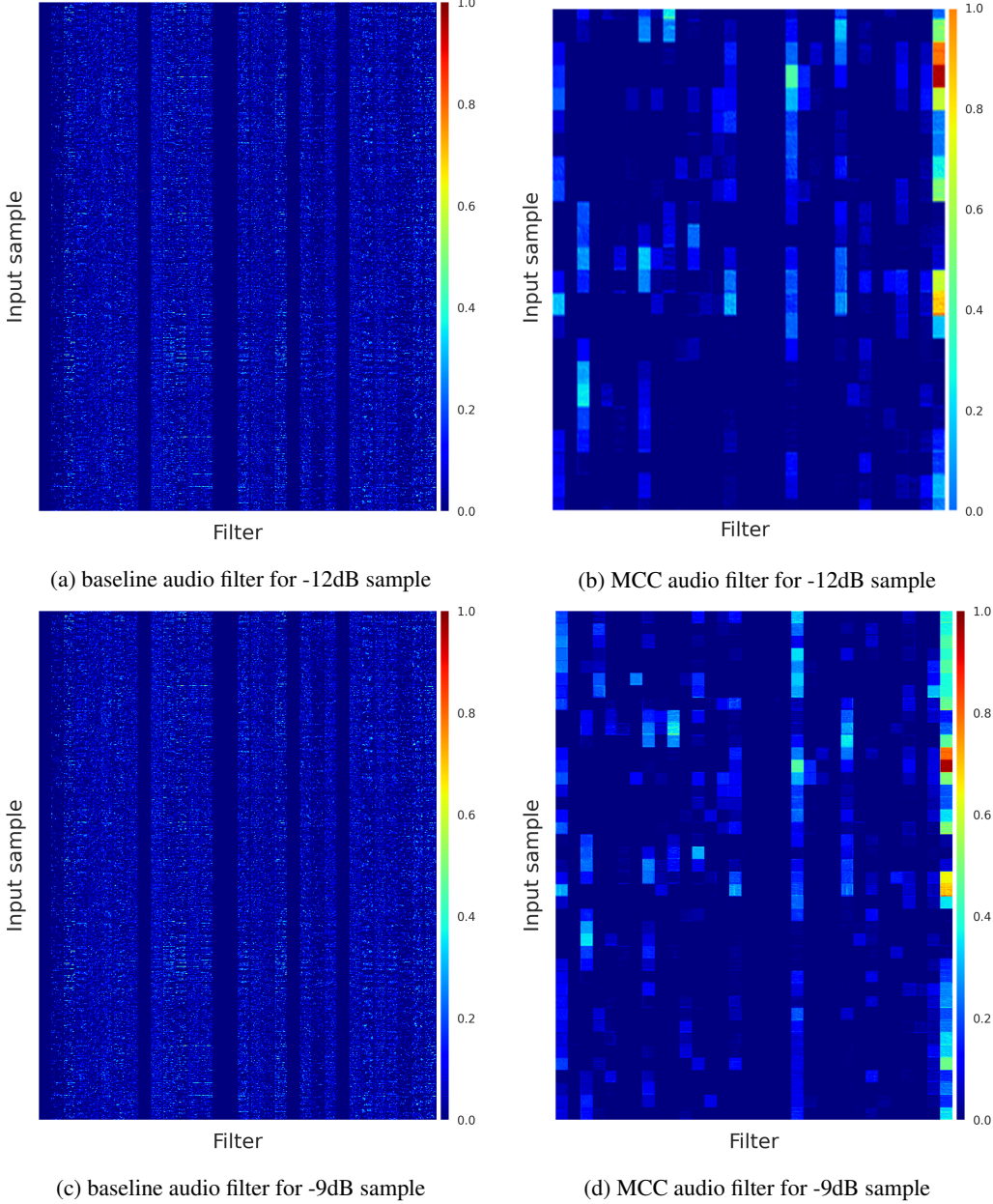


Figure 6: Amplification of relevant signals and suppression of irrelevant signals: In MCC, different filters across the rows indicate what matters when. In contrast, the baseline treats each input equally, ignoring the variant information across the time. Note that MCC uses a full range of available frequency spectrum e.g., filters in red, green, blue, and orange emphasise the level of relevance, whereas the irrelevant neurons are off. It is worth mentioning that MCC is able to construct high-level features at low-level layers requiring less number of layers to construct a good representation. In contrast, the baseline requires more layers and more resources to do so. The Y-axis represents the input signal of 240ms duration, where each small block is of 10ms duration. The X-axis represents 32 convolutional filters.

all the incoming streams in an identical way i.e., simply summing up all the excitatory and inhibitory inputs with an assumption that they have the same chance of affecting the neuron's output [1].

Figure 6 reveals the selective amplification and suppres-

sion property of the proposed MCC. The baseline treats each input with equal importance and computes features regardless of the underlying nature of the signal. On the contrary, MCC can highlight relevant and irrelevant features. This analysis could also be seen as a Fourier analysis

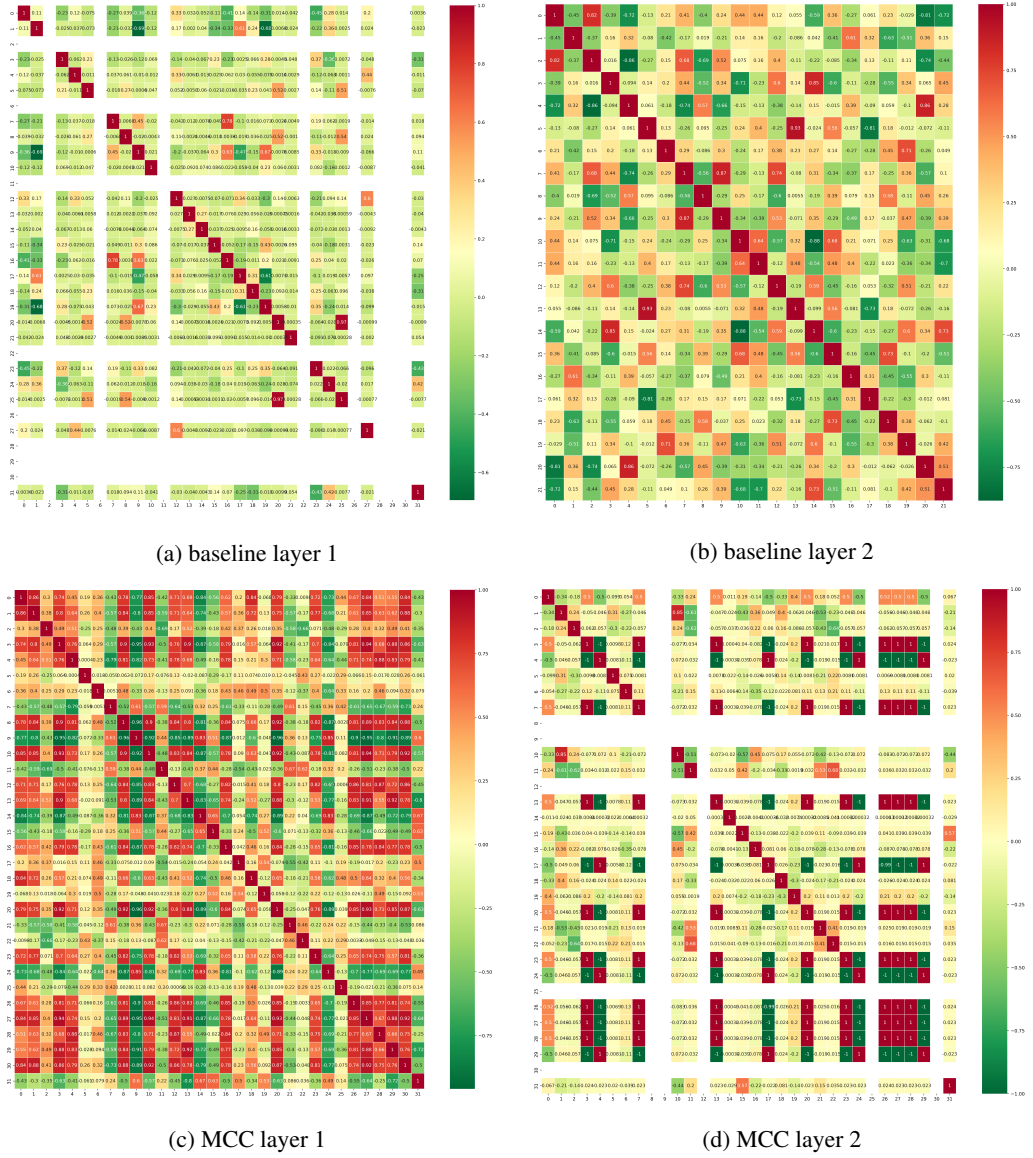


Figure 7: Relevant data transmission: The data from 32 neurons show that MCC reduces the cross-correlation as the data passes through different layers. MCC is also able to discover a statistical structure that is far more definite beginning from layer 1 (c) and becoming even clearer in layer 2 (d) e.g., a block of 4 cells in the bottom right corner.

or time-frequency analysis explaining what matters when. We hypothesise that MCC is highlighting which phonemes matter the most, or discovering the aspects of speech that can be seen in the video or discovering the structure (high-level features) at early layers. These results also show that neurons in MCC have more cognitive ability to make important decisions at the cellular level. In general, these patterns are certainly providing important information as compared to the baseline. In Figure 6d, although the filters that matter remain marginally the same but the extent to when they matter vary depending upon the noise.

Figure 7 depicts how the data is statistically transformed

through different MCC layers compared to the baseline model. The autocorrelation and cross-correlation data from 32 neurons are shown. It can be seen that cross-correlation reduces significantly in MCC when moving from one layer to the next i.e., more information passed on to the next block. In contrast, the baseline passes more redundant data to the next layer as high cross-correlation could be observed. Figure 8 depicts the effect of selective information processing on learning speed (Figure 8a), neural activity (Figure 8b), and generalisation (Figures 8c). It is to be noted that MCC with energy term learns faster and achieves best reconstruction with a significantly

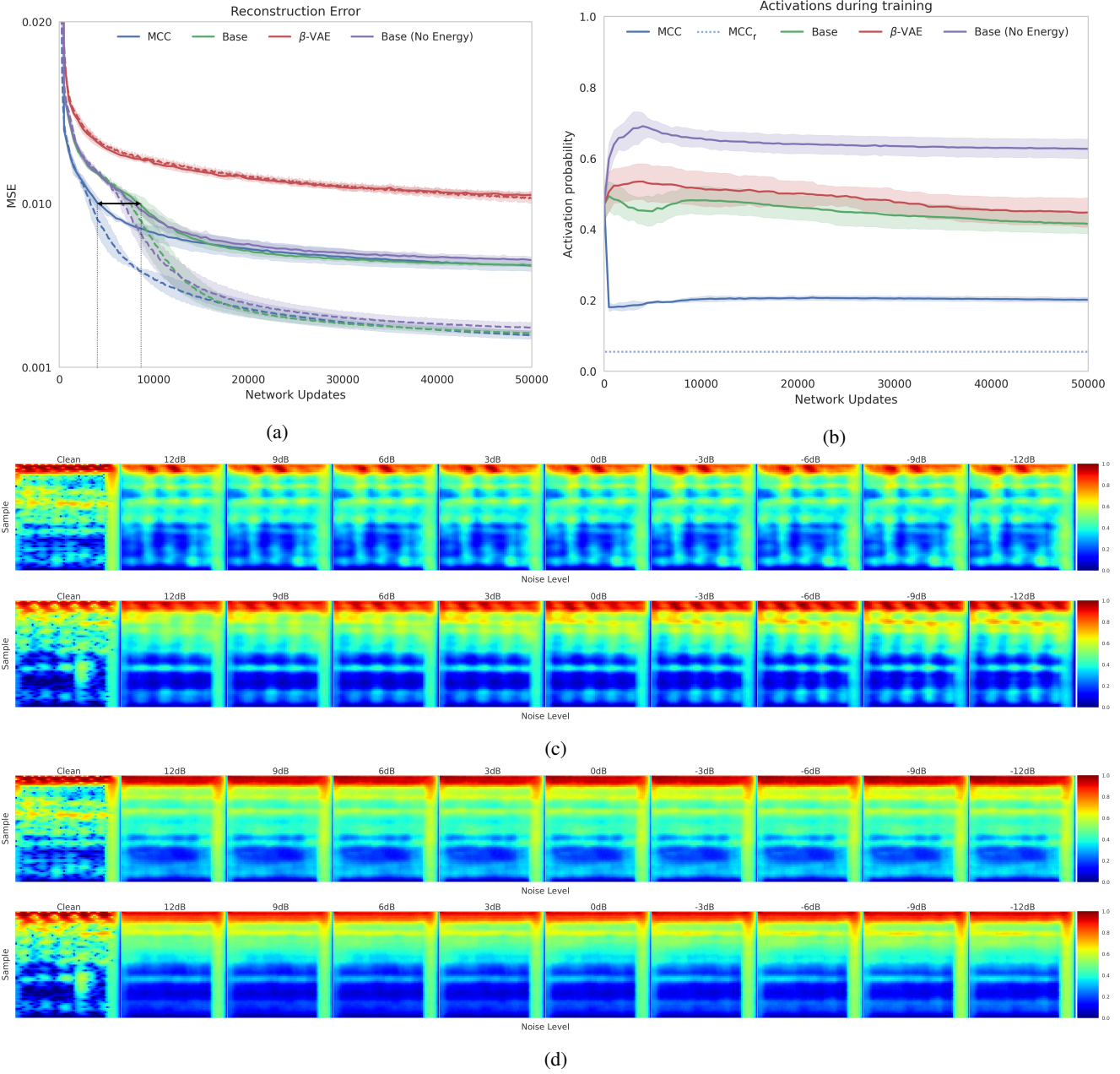


Figure 8: Task 1: (a) Semi-supervised reconstruction error and (b) its respective firing evolution. Neurons in MCC quickly evolve to become highly sensitive to relevant information and become active only when the received information is important for the task at hand. Thus, MCC can separate clean speech from large amounts of noise using far fewer neurons e.g., trained MCC with 35% randomly killed neurons (MCC_r) during testing could reconstruct clean speech with approx., 4% overall neural activity and MSE of 0.01 (see ‘Methods’ for more details) (c-d) clean-signal reconstruction for different levels of noise. It is to be noted that MCC (c) captures high-frequency features more easily compared to the baseline (d). Solid and dashed lines indicate testing loss and training loss, respectively.

reduced neural activity. This efficient processing is due to context-sensitive activity at the cellular level that enables the network to identify most relevant features at very early stages in the network. Specifically, the individual

neurons quickly evolve to become highly sensitive to a specific type of high-level information, allowing them to be selective as to what data is worth paying attention to and therefore processing just that, instead of having

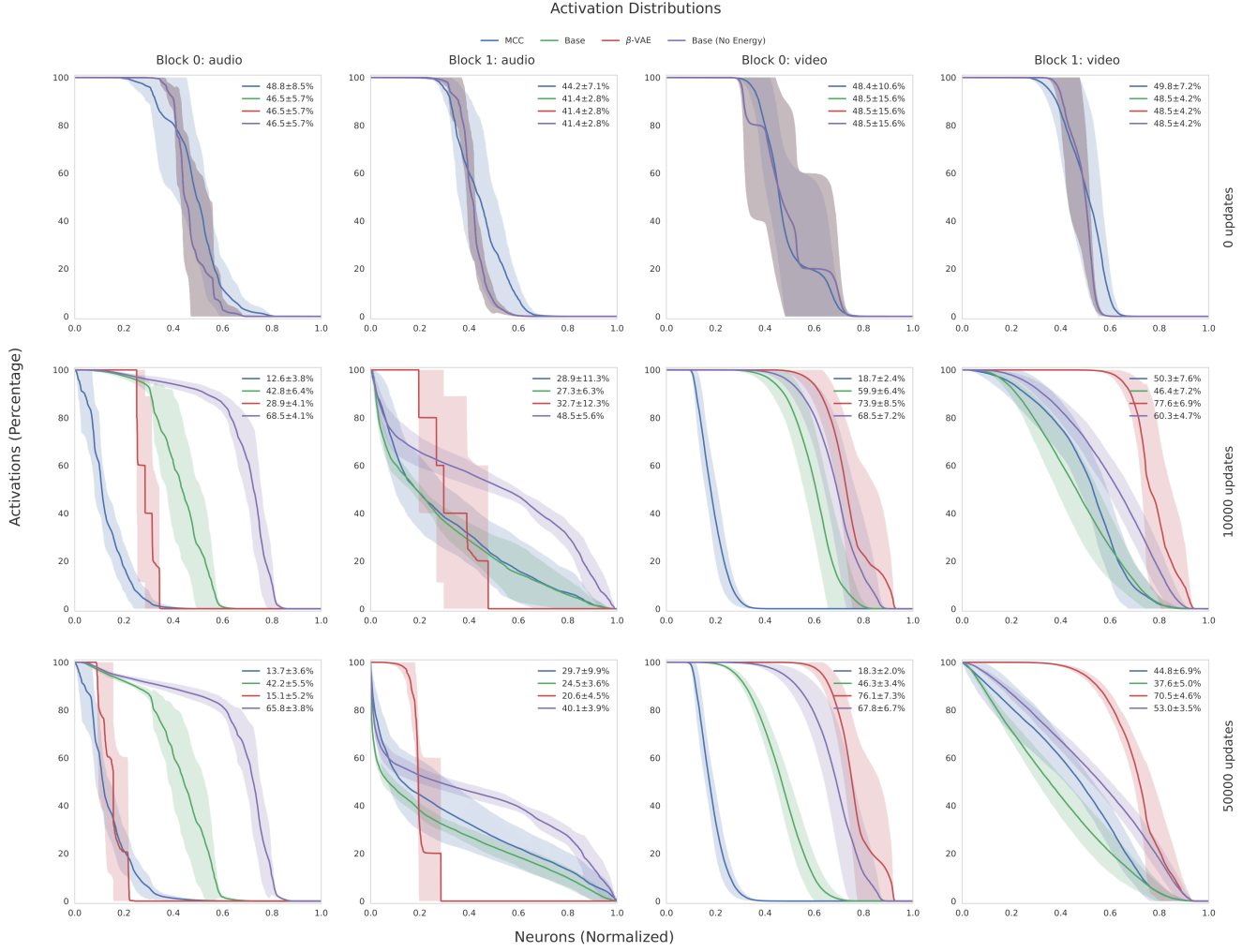


Figure 9: Neural activity: MCC reaches the low neural activity 10X faster than the baseline model. For example, see row 2, column 3. The X-axis represents a neuron’s firing probability.

to process everything. This reduction in neural activity is equivalent to a magnitude of energy efficiency during training if the synapses associated with the cells with zero activity are turned off in the hardware. Figure 9 depicts a more detailed neural firing behaviour over time. It can be seen that MCC converges to the lower neural activity approx., 10X faster than the baseline model. The quality of reconstruction with MCC (Figure 8c) is sensitive to fine-grained details and distinguishes the relevant signal more easily and clearly. This may have a significant impact on the reconstructed time-domain speech signal and its intelligibility [36]. Although, the β -VAE model converges to a low neural activity level compared to the Base without energy term but with low reconstruction quality. The baseline model with and without energy constraint achieves a lower reconstruction error with significantly higher neural activity.

Similarly, for multimodal (MM) representation learning via estimating and maximizing the mutual information (MI) between high dimensional clean visual and noisy speech signals (Figure 10a), the baseline models remain deficient in achieving high MI, regardless of the experimental setup, hyper-parameters, and loss function. Figure 10c depicts the MI estimation and maximization for empirical multivariate Gaussian random variables (GRVs). We compare MCC with mutual information neural estimator (MINE), MINE f-divergence (MINE-f), and density ratio [42]. MCC shows marked improvement overall when estimating the MI between twenty-dimensional GRVs. We also remark that MCC converges quickly to the true MI. When MCC is applied to reconstruct high-dimensional clean speech in a supervised fashion using mask estimation [43], it works remarkably well (Figure 11). The comparative simulation results of speech quality and intelligibility

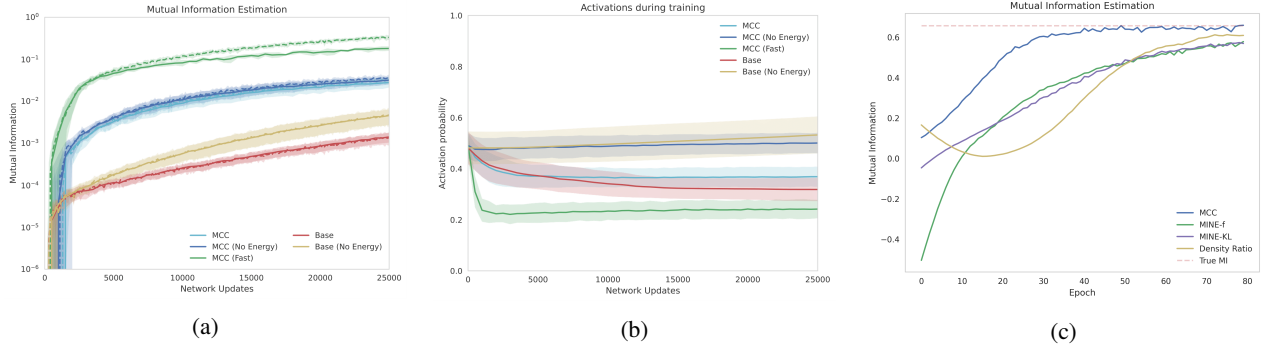


Figure 10: Task 2: (a) Unsupervised MI estimation and maximization between high dimensional clean visual and noisy speech signal (b) and its respective firing evolution. The baseline cannot handle high learning rates. In contrast, MCC (fast) uses a learning rate one order of magnitude bigger than the rest without collapsing. Solid and dashed lines indicate testing loss and training loss, respectively. Note that MCC converges quickly to the higher/true MI with a significantly reduced neural activity.

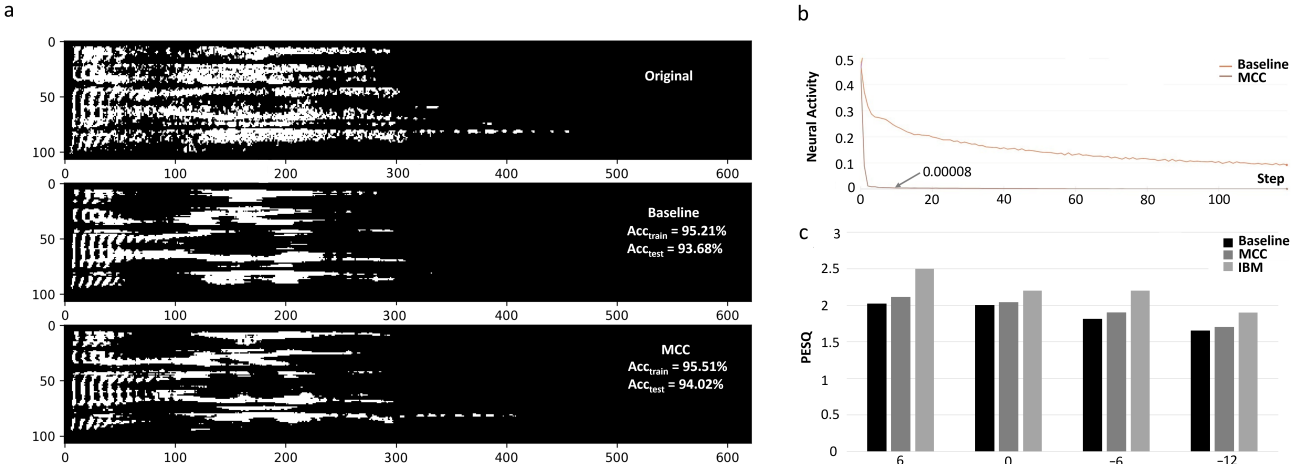


Figure 11: Task 3: Supervised reconstruction accuracy (mask estimation (a)) and (b) its respective firing evolution. Individual neurons in MCC reduce their neural activity far more quickly in supervised reconstruction than baseline model. Specifically, MCC neurons can effectively process large amounts of heterogeneous real-world AV data with an overall neural activity of less than 0.008% i.e., 1250x less (per FF transmission) than point neurons. More remarkably, these neurons quickly evolve and reach this low neural activity in just three training updates, which further increases the efficiency of MCC. Here the models are trained for 50,000 updates, therefore, the efficiency is $\approx 50,000$ multiplied by 1250x. Along with this very minimal neural activity, these neurons can successfully reconstruct high-dimensional clean speech corrupted by multiple real-world noises in real-world like conditions (see mask estimation in (a) and resulting perceptual evaluation of speech quality (PESQ) in (c)). PESQ score is objectively measuring the quality of re-synthesised speech. It can be seen that MCC, despite its very low neural activity, can reconstruct the speech better than the baseline model - closer to the ideal binary mask (IBM) (see ‘Methods’).

demonstrate that individual neurons in MCC significantly reduce their neural activity in just a few training epochs and reconstruct speech better than the baseline state-of-the-art DNN model [43].

Discussion

Results show that the proposed biologically plausible co-operative context-sensitive style of information processing, supported by the latest and rapidly growing neurobiological

discoveries on two-point cells, may be fundamental to the capabilities of the mammalian neocortex. The context sensitivity at the cellular level indeed has information processing abilities of the kind displayed by the mammalian neocortex.

Results also show that the fundamental weakness of state-of-the-art deep learning [44] is its dependence on a long-established simplified point neural model that

maximizes the transmission of information irrespective of whether or not the information is useful to other neurons or for the long-term benefit of the whole network. This mechanism leads to unnecessary neural firing and conflicting messages to higher perceptual layers making DNNs energy-inefficient and hard to train.

Although point neurons allow DNNs to learn the representation of information with multiple levels of abstraction, their processing is shallow [45]. These neurons encode the FF information based on repetition activity (learning) without any search for coherence. In contrast, our proposed cooperative context-sensitive neural information processing promotes deep information processing (DIP) [45] that allows individual neurons to have more deeper and well-reasoned interaction with the received FF information. Individual neurons cooperate moment-by-moment and fire only when the received FF information is coherent to the overall activity of the network or relevant to the task at hand. This enables relevant feature extraction at very early stages in the network, leading to faster learning, reduced neural activity, and enhanced resilience.

To the best of our knowledge, this is the first time context-sensitive two-point L5PC mechanism has been applied to solve any challenging real-world problem, reflecting its potential to transform the capabilities of neurocomputational systems. Although a few experts in machine learning such as G. Hinton [46], T.P. Lillicrap [47], R. Naud [48], and Y. Bengio [49] have been inspired by these neurobiological discoveries, they do not interpret them as evidence for two-point neurons as we do here. Specifically, their papers have focused predominantly on learning, whereas our paper is predominantly focused on using context to guide ongoing processing. Therefore, we are able to develop new forms of context-sensitive information processing mechanisms that can outperform the best available forms of deep learning inspired by the ‘point’ neuron assumption. Overall, the proposed model is more closely based on neuroscience and psychology than other deep learning algorithms, so it is more likely to reflect the way our minds work. We believe that the proposed work represents a radical advance beyond existing forms of machine learning and could be a major advantage in real-world applications where speed and the efficient use of energy are important.

It is worth mentioning that our work is not only a model. It is more important than that. It is a demonstration that the cooperative context-sensitive style of neural information processing works and is far more effective and efficient than the best available forms of neural information processing algorithms. Our contribution to this rapidly growing field of research encourages neurobiologists to search for the essentials (fine-tunings) which were necessary to make this neurobiological mechanism work. We learnt that it is critical to understand the formation of different kinds of

contexts arriving at the apical tuft and how exactly they influence the cell’s response to the FF input e.g., how conditional segregation and recombination of multiple input streams transform into brief memory and how the broadcasted content of brief memory (universal context) along with the local context play an important role in selective amplification and suppression of relevant and irrelevant signals, respectively.

The demonstration of relevant signals amplification and irrelevant signals suppression and the construction of high-level features at low-level layers shed light on the cognitive ability of low-level layers (at the cellular level) that is higher than the high-level layers. Specifically, we show how low-level layers can make strategic decisions and restrict the transmission of conflicting features to the higher layers to avoid disorganization.

The proposed work also bridges the gap between Dendritic Integration Theory [26] and Global Neuronal Workspace Theory [29] e.g., the notion of universal context matches with the universal role of the NSP-thalamus whose modulatory effect is broadcasted to all sensory modalities activating other brain areas [30]. We suggest that in addition to the synergy between apical and basal information flow in L5PC [22], the synergy between different coherent information streams (i.e., universal context) could be closely related to conscious experience. Whether this holds true or not, the role of universal context is of great importance since things are experienced differently in positive and negative frames of mind and with different intentions, attentions, hopes, and emotional states.

We suggest that the universal context may be analogous to signals that regulate the balance between apical/internal/top-down/feedback and basal/external/sensory/feedforward inputs. Thus, switching the mode of apical function between amplification (or drive) and isolation. If so, the idea of the universal context may be relevant to a major physiological process that is only now being seen to be important [24][27]. Finally, the notion of universal context leads us to think that the ‘self’ is an enduring part of the internal context. So, are ‘we’ the enduring internal context within which our experiences occur? We also hypothesise that contextual signals are formed through conditional segregating and reintegration, and context can overrule the typical dominance of the FF input.

The proposed work could also help to better understand neurodevelopmental disorders such as autism and sensory overload when early brain layers fail to filter out irrelevant information and the brain becomes overwhelmed due to excessive contradictory messages transmitted to higher perceptual levels [50][51], or epilepsy when the bursts of electrical activity in the brain cause seizures. Last but not least, the proposed work sheds light on human’s basic

cooperative instinct that achieves harmony via organized cooperation between diverse neurons [52][53][54]. In general, the presented work is important for biology because it is inspired by the latest and rapidly growing fundamental advances in cellular neurobiology thus can open the door to exciting new opportunities in neurobiology, neurobiotechnology, and neurocomputational technology. Furthermore, it supports the argument that the leaky integrate-and-fire (LIF) conception of the neuron harms our progress in understanding brain function [8].

Although the proposed cooperative context-sensitive style of information processing is biologically plausible, the learning is still based on backpropagation. Future work involves using local context as a feedback error e.g., for credit assignment, as opposed to the way it is typically used for training standard deep learning algorithms [47][48]. We aim to provide further insights into cooperative context-sensitive information learning mechanism. Ongoing work also involves the demonstration of the proposed modulatory concept within unimodal streams to extend cooperative context-sensitive information processing well beyond multimodal applications.

Methods

Simulation details: For a fair comparison, all deep models have a similar structure, layers, and configuration. We used two convolutional layers, each with 32 filters, kernels of size 5 and stride 2. For each channel embedding, we used 128 units and for the global embedding, we used 256 units. Additional terms to the losses, like ELBO loss, were added to the loss function model-wise. All activation functions are ReLUs. All networks are initialized with a glorot uniform distribution. The Adam optimizer with a learning rate of $1e^{-6}$ and $1e^{-4}$ is used for all the experiments. Although we do not claim these configurations are optimal, we empirically observed models behaved well with this set of parameters.

Each element of the dataset is a tuple containing a noisy audio signal (STFT), a snapshot of the lips of the speaker (image), and a clean audio signal (STFT). The SNR varies from +12dB to -12dB in steps of 3dB. As usual in machine learning, we take a split 80%-20% for training and testing; we leave a single sample out of training and testing splits to use as a proxy for the figures in this work. Data is normalized across the whole dataset and presorted to break all order correlations. The dataset is shuffled once more with a seed to add some variability between different runs and to ensure that different models encounter a similar landscape. We use a mini-batch size of 256 for all the experiments. The average was taken from 5 different runs, using the same seeds for different models.

For MI estimation and speech denoising we used the

following loss functions:

$$\begin{aligned}\mathcal{L}_1 &= -\alpha \mathbb{E} [-I_f(\mathbf{X}; \mathbf{Y})] + \gamma \mathbb{E} [\mathcal{E}] \\ \mathcal{L}_2 &= \beta \mathbb{E} [\text{SE}(\mathbf{Z}, \hat{\mathbf{Z}})] + \gamma \mathbb{E} [\mathcal{E}]\end{aligned}$$

\mathcal{E} is a differentiable approximation for the number of firings. We adjust the coefficients of the loss functions to make the secondary objectives significantly less important than the main goal; in particular, we set γ to a really small value in all experiments. We set $\gamma = 0$ for the task (1) for the baseline since it may randomly shut down after a couple of updates. Even for very small γ , we encounter that the gradient signal from the energy may be several orders of magnitude greater than the signal originated from the MI estimation.

Speech denoising: The noisy audio was corrupted with several different noise sources. Although, more sophisticated approaches for denoising using neural networks exist, our goal is to measure the capabilities of the network using as few resources as possible (neural activity). For this experiment, we introduced a small change into the modulatory step, in which we also take the activity of neighbouring neurons into account twice, once when we compute the context and again when we apply the modulation. This small change is equivalent to replacing the delta operator of equation 6.

MI estimation: MM representation learning via MI maximization has proven to significantly improve both the classification and regression tasks [42][55][56]. However, MI maximization between high dimensional input variables in the presence of extreme noise is a serious challenge. Here we pose a problem of learning MM representation via estimating and maximizing the MI between high dimensional clean visual and noisy speech signals. For direct computation of the entropy or the Kullback–Leibler divergence, we use Donsker–Varadhan representation. In other words, we transformed the mutual information estimation problem into an optimization problem [42].

Consider $\mathbf{X}_\alpha \in V_\alpha$ and $\mathbf{Y}_\beta \in V_\beta$ two random multi-dimensional variables indexed by $\alpha \in \{1, \dots, A\}$, $\beta \in \{1, \dots, B\}$, with $V_\alpha \subseteq \mathbb{R}^A$ and $V_\beta \subseteq \mathbb{R}^B$ and distributed as \mathbb{P}_X and \mathbb{P}_Y , respectively.

The mutual information between these two variables, $I(\mathbf{X}_\alpha; \mathbf{Y}_\beta)$, is given by,

$$I(\mathbf{X}_\alpha; \mathbf{Y}_\beta) = H(\mathbf{X}_\alpha) - H(\mathbf{X}_\alpha | \mathbf{Y}_\beta) = \mathcal{D}_{KL}(\mathbb{P}_X \parallel \mathbb{P}_Y)$$

In general, direct computation of the entropy or the Kullback–Leibler divergence is not feasible. Fortunately, it is possible to rewrite this expression using the Donsker–Varadhan representation. Thus,

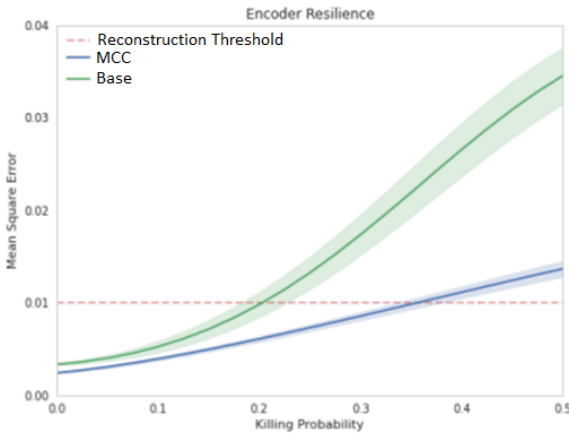


Figure 12: Resilience test: the performance degrades gracefully in MCC as compared to the baseline. MCC can achieve good accuracy with approx., 4% overall neural activity.

$$\begin{aligned}
 I(\mathbf{X}_\alpha; \mathbf{Y}_\beta) &= \sup_{f \in \mathcal{F}} I_f(\mathbf{X}_\alpha; \mathbf{Y}_\beta) \\
 &= \sup_{f \in \mathcal{F}} \mathbb{E}_{\mathbb{P}_{XY}} [f(\mathbf{X}_\alpha, \mathbf{Y}_\beta)] \\
 &\quad - \log (\mathbb{E}_{\mathbb{P}_X \times \mathbb{P}_Y} [\exp(f(\mathbf{X}_\alpha, \mathbf{Y}_\beta))]) \quad (8)
 \end{aligned}$$

where \mathcal{F} is a set of functions $f : V_\alpha \times V_\beta \mapsto \mathbb{R}$ with finite expectations under \mathbb{P}_{XY} and $\mathbb{P}_X \times \mathbb{P}_Y$.

Hence, $\forall f \in \mathcal{F}$ we have:

$$I(\mathbf{X}_\alpha; \mathbf{Y}_\beta) \geq I_f(\mathbf{X}_\alpha; \mathbf{Y}_\beta) \quad (9)$$

Deep multimodal supervised reconstruction: For this task, we used the mask estimation approach for speech enhancement presented in [43][37].

AV corpus: For AV speech processing, the Grid [57] and ChiME3 [58] corpora are used [36], including four different noise types; cafe, street junction, public transport (bus), and pedestrian area with the signal-to-noise ratio (SNRs) ranging from -12dB to 12dB with a step size of three. Grid and ChiME3 corpora are publicly available and open-source, thus, ethical approval is not needed, including speakers in Figure 6 that are from another open-source AV dataset [59].

Auto-correlation and cross-correlation analysis: For this analysis, a semi-supervised AV speech processing with the shallow MCC and baseline model is analysed. In this experimental setup, logFB audio features of dimension 22 and DCT visual features of dimension 50 were used [60].

Resilience test: Random neurons are killed (set to zero) with a probability P . To make the comparison as fair as possible, only neurons from the convolutional layers are killed.

Points are estimated from $P=0$ to 0.5 with steps of 0.025. We observe the whole testing dataset 50 times per point. The average/standard deviation is taken from the 5 runs of each model. It can be seen in Figure 12 that MCC has significantly better resistance to neuron damage. This is due to the fact that our model highlights the important features given the nature of the input, and does not look at the input processed features without any vis a vis importance or weight of the features. Empirically, we observe that the quality of the reconstruction drastically decreases when going above the 0.01 error.

Decoder details: The decoder's initial layer is a fully connected layer followed by an (8,8,64) reshape. We apply four transpose convolutional transformations with 64, 32, 16 and 1 filters respectively. Kernel size is 3, the stride is 2 for all four convolutional steps. Activation function is ReLU. Batch normalization is added prior to each ReLU to enhance even further learning speed. The decoder's network is initialized with a glorot uniform distribution. This simple decoder is enough to achieve an almost perfect reconstruction when provided with the clean input in just a matter of a few updates (data not shown). Thus, the final quality of the reconstruction is entirely dependent on the quality of the features provided by the encoder. Additional decoders required by the autoencoders have a similar structure.

Acknowledgments This research was supported by the UK Engineering and Physical Sciences Research Council (EPSRC) Grant Ref. EP/T021063/1. We would like to acknowledge Professor Bill Phillips from the University of Stirling, Dr James Kay from the University of Glasgow, and Professor Newton Howard from Oxford Computational Neuroscience for their help and support in several different ways, including reviewing our work, appreciation, motivation, and encouragement.

Contributions AA conceived and developed the original idea, wrote the manuscript, and analysed the results. AA, MF, MR, and KA performed the simulations.

Competing interests AA has a provisional patent application for the algorithm described in this article. The other authors declare no competing interests.

References

- [1] M. Häusser, "Synaptic function: Dendritic democracy," *Current Biology*, vol. 11, no. 1, pp. R10–R12, 2001.
- [2] A. Burkitt, "A review of the integrate-and-fire neuron model: I. homogeneous synaptic input," *Biological cybernetics*, vol. 95, pp. 1–19, 08 2006.
- [3] M. E. Larkum, J. J. Zhu, and B. Sakmann, "A new cellular mechanism for coupling inputs arriving at different cortical layers," *Nature*, vol. 398, no. 6725, pp. 338–341, 1999.

- [4] M. Larkum, “A cellular mechanism for cortical associations: an organizing principle for the cerebral cortex,” *Trends in neurosciences*, vol. 36, no. 3, pp. 141–151, 2013.
- [5] G. Major, M. E. Larkum, and J. Schiller, “Active properties of neocortical pyramidal neuron dendrites,” *Annual review of neuroscience*, vol. 36, pp. 1–24, 2013.
- [6] S. Ramaswamy and H. Markram, “Anatomy and physiology of the thick-tufted layer 5 pyramidal neuron,” *Frontiers in cellular neuroscience*, vol. 9, p. 233, 2015.
- [7] W. A. Phillips, “Cognitive functions of intracellular mechanisms for contextual amplification,” *Brain and Cognition*, vol. 112, pp. 39–53, 2017.
- [8] M. E. Larkum, “Are dendrites conceptually useful?” *Neuroscience*, vol. 489, pp. 4–14, 2022.
- [9] J. M. Shine, P. G. Bissett, P. T. Bell, O. Koyejo, J. H. Balsters, K. J. Gorgolewski, C. A. Moodie, and R. A. Poldrack, “The dynamics of functional brain networks: integrated network states during cognitive task performance,” *Neuron*, vol. 92, no. 2, pp. 544–554, 2016.
- [10] J. M. Shine, M. Breakspear, P. T. Bell, K. A. Ehgoetz Martens, R. Shine, O. Koyejo, O. Sporns, and R. A. Poldrack, “Human cognition involves the dynamic integration of neural activity and neuromodulatory systems,” *Nature neuroscience*, vol. 22, no. 2, pp. 289–296, 2019.
- [11] J. M. Shine, “Neuromodulatory influences on integration and segregation in the brain,” *Trends in cognitive sciences*, vol. 23, no. 7, pp. 572–583, 2019.
- [12] J. M. Shine, E. J. Müller, B. Munn, J. Cabral, R. J. Moran, and M. Breakspear, “Computational models link cellular mechanisms of neuromodulation to large-scale neural dynamics,” *Nature neuroscience*, vol. 24, no. 6, pp. 765–776, 2021.
- [13] B. Schuman, S. Dellal, A. Prönneke, R. Machold, and B. Rudy, “Neocortical layer 1: An elegant solution to top-down and bottom-up integration,” *Annual Review of Neuroscience*, vol. 44, no. 1, pp. 221–252, 2021, pMID: 33730511.
- [14] P. Poirazi and A. Papoutsi, “Illuminating dendritic function with computational models,” *Nature Reviews Neuroscience*, vol. 21, pp. 1–19, 05 2020.
- [15] M. E. Larkum, L. S. Petro, R. N. Sachdev, and L. Muckli, “A perspective on cortical layering and layer-spanning neuronal elements,” *Frontiers in neuroanatomy*, vol. 12, p. 56, 2018.
- [16] J. M. Schulz, J. W. Kay, J. Bischofberger, and M. E. Larkum, “Gaba b receptor-mediated regulation of dendro-somatic synergy in layer 5 pyramidal neurons,” *Frontiers in cellular neuroscience*, vol. 15, p. 718413, 2021.
- [17] J. W. Kay and W. A. Phillips, “Contextual modulation in mammalian neocortex is asymmetric,” *Symmetry*, vol. 12, no. 5, p. 815, 2020.
- [18] J. W. Kay, J. M. Schulz, and W. A. Phillips, “A comparison of partial information decompositions using data from real and simulated layer 5b pyramidal cells,” *Entropy (in press); preprint at <http://arxiv.org/abs/2206.06456>*, 2022.
- [19] M. L. Tantirigama, T. Zolnik, B. Judkewitz, M. E. Larkum, and R. N. Sachdev, “Perspective on the multiple pathways to changing brain states,” *Frontiers in Systems Neuroscience*, vol. 14, p. 23, 2020.
- [20] A. D. Nelson and K. J. Bender, “Dendritic integration dysfunction in neurodevelopmental disorders,” *Developmental Neuroscience*, vol. 43, no. 3-4, pp. 201–221, 2021.
- [21] J. Aru, M. Suzuki, R. Rutiku, M. E. Larkum, and T. Bachmann, “Coupling the state and contents of consciousness,” *Frontiers in Systems Neuroscience*, vol. 13, p. 43, 2019.
- [22] J. Aru, M. Suzuki, and M. Larkum, “Cellular mechanisms of conscious processing,” *Trends in Cognitive Sciences*, vol. 25, 10 2021.
- [23] G. M. Shepherd and N. Yamawaki, “Untangling the cortico-thalamo-cortical loop: cellular pieces of a knotty circuit puzzle,” *Nature Reviews Neuroscience*, vol. 22, no. 7, pp. 389–406, 2021.
- [24] T. Marvan, M. Polák, T. Bachmann, and W. A. Phillips, “Apical amplification—a cellular mechanism of conscious perception?” *Neuroscience of consciousness*, vol. 2021, no. 2, p. niab036, 2021.
- [25] A. Adeel, “Conscious multisensory integration: Introducing a universal contextual field in biological and deep artificial neural networks,” *Frontiers in Computational Neuroscience*, vol. 14, 05 2020.
- [26] T. Bachmann, M. Suzuki, and J. Aru, “Dendritic integration theory: a thalamo-cortical theory of state and content of consciousness,” *Philosophy and the Mind Sciences*, vol. 1, no. II, 2020.
- [27] J. Shin, G. Doron, and M. Larkum, “Memories off the top of your head,” *Science*, vol. 374, pp. 538–539, 10 2021.

- [28] B. Schuman, S. Dellal, A. Prönneke, R. Machold, and B. Rudy, “Neocortical layer 1: An elegant solution to top-down and bottom-up integration,” *Annual Review of Neuroscience*, vol. 44, no. 1, pp. 221–252, 2021, pMID: 33730511.
- [29] B. Baars, “Global workspace theory of consciousness: Toward a cognitive neuroscience of human experience,” *Progress in brain research*, vol. 150, pp. 45–53, 02 2005.
- [30] A. Vasconcelos and J.-C. Cassel, “The nonspecific thalamus: A place in a wedding bed for making memories last?” *Neuroscience & Biobehavioral Reviews*, vol. 54, 11 2014.
- [31] D. J. Heeger and W. E. Mackey, “Oscillatory recurrent gated neural integrator circuits (organics), a unifying theoretical framework for neural dynamics,” *Proceedings of the National Academy of Sciences*, vol. 116, no. 45, pp. 22 783–22 794, 2019.
- [32] D. J. Heeger and K. O. Zemlianova, “A recurrent circuit implements normalization, simulating the dynamics of v1 activity,” *Proceedings of the National Academy of Sciences*, vol. 117, no. 36, pp. 22 494–22 505, 2020.
- [33] T. Bachmann and A. G. Hudetz, “It is time to combine the two main traditions in the research on the neural correlates of consciousness: $C = 1 \times d$,” *Frontiers in Psychology*, vol. 5, p. 940, 2014.
- [34] W. A. Phillips, T. Bachmann, and J. F. Storm, “Apical function in neocortical pyramidal cells: a common pathway by which general anesthetics can affect mental state,” *Frontiers in neural circuits*, vol. 12, p. 50, 2018.
- [35] A. Adeel, “Multistream cooperative context-sensitive neural information processing,” *UK Patent application, GB2119011.1*, 2021.
- [36] A. Adeel, M. Gogate, and A. Hussain, “Contextual deep learning-based audio-visual switching for speech enhancement in real-world environments,” *Information Fusion*, vol. 59, 08 2019.
- [37] M. Gogate, K. Dashtipour, A. Adeel, and A. Hussain, “Cochleanet: A robust language-independent audio-visual model for speech enhancement,” *Information Fusion*, vol. 63, 04 2020.
- [38] J. Yang, Z. Ren, C. Gan, H. Zhu, and D. Parikh, “Cross-channel communication networks,” *Advances in Neural Information Processing Systems*, vol. 32, 2019.
- [39] C. Cangea, P. Veličković, and P. Lio, “Xflow: Cross-modal deep neural networks for audiovisual classification,” *IEEE Transactions on Neural Networks and Learning Systems*, vol. 31, no. 9, pp. 3711–3720, 2019.
- [40] W. Guo, J. Wang, and S. Wang, “Deep multimodal representation learning: A survey,” *IEEE Access*, vol. PP, pp. 1–1, 05 2019.
- [41] A. Bhatti, B. Behinaein, D. Rodenburg, P. Hungler, and A. Etemad, “Attentive cross-modal connections for deep multimodal wearable-based emotion recognition,” in *2021 9th International Conference on Affective Computing and Intelligent Interaction Workshops and Demos (ACIIW)*. IEEE, 2021, pp. 01–05.
- [42] M. I. Belghazi, A. Baratin, S. Rajeshwar, S. Ozair, Y. Bengio, A. Courville, and D. Hjelm, “Mutual information neural estimation,” in *International conference on machine learning*. PMLR, 2018, pp. 531–540.
- [43] M. Gogate, A. Adeel, R. Marxer, J. Barker, and A. Hussain, “Dnn driven speaker independent audio-visual mask estimation for speech separation,” in *Interspeech 2018*. ISCA, 2018, pp. 2723–2727.
- [44] Y. LeCun, Y. Bengio, and G. Hinton, “Deep learning,” *nature*, vol. 521, no. 7553, pp. 436–444, 2015.
- [45] F. I. Craik and R. S. Lockhart, “Levels of processing: A framework for memory research,” *Journal of Verbal Learning and Verbal Behavior*, vol. 11, no. 6, pp. 671–684, 1972.
- [46] T. Lillicrap, A. Santoro, L. Marris, C. Akerman, and G. Hinton, “Backpropagation and the brain,” *Nature Reviews Neuroscience*, vol. 21, 04 2020.
- [47] J. Guerguiev, T. Lillicrap, and B. Richards, “Towards deep learning with segregated dendrites,” *eLife*, vol. 6, p. e22901, 12 2017.
- [48] A. Payeur, J. Guerguiev, F. Zenke, B. A. Richards, and R. Naud, “Burst-dependent synaptic plasticity can coordinate learning in hierarchical circuits,” *Nature neuroscience*, vol. 24, no. 7, pp. 1010–1019, 2021.
- [49] J. Sacramento, R. Ponte Costa, Y. Bengio, and W. Senn, “Dendritic cortical microcircuits approximate the backpropagation algorithm,” *Advances in neural information processing systems*, vol. 31, 2018.
- [50] T. Rinaldi, C. Perrodin, and H. Markram, “Hyper-connectivity and hyper-plasticity in the medial pre-frontal cortex in the valproic acid animal model of autism,” *Frontiers in neural circuits*, vol. 2, p. 4, 2008.

- [51] K. Markram and H. Markram, “The intense world theory—a unifying theory of the neurobiology of autism,” *Frontiers in human neuroscience*, p. 224, 2010.
- [52] M. Ridley and F. B. d. Waal, “The origins of virtue,” *Nature*, vol. 383, no. 6603, pp. 785–785, 1996.
- [53] J. K. Rilling, D. A. Gutman, T. R. Zeh, G. Pagnoni, G. S. Berns, and C. D. Kilts, “A neural basis for social cooperation,” *Neuron*, vol. 35, no. 2, pp. 395–405, 2002.
- [54] A. Delle Fave, I. Brdar, M. P. Wissing, U. Araujo, A. Castro Solano, T. Freire, M. D. R. Hernández-Pozo, P. Jose, T. Martos, H. E. Nafstad *et al.*, “Lay definitions of happiness across nations: The primacy of inner harmony and relational connectedness,” *Frontiers in psychology*, vol. 7, p. 30, 2016.
- [55] P. Velickovic, W. Fedus, W. L. Hamilton, P. Liò, Y. Bengio, and R. D. Hjelm, “Deep graph infomax.” *ICLR (Poster)*, vol. 2, no. 3, p. 4, 2019.
- [56] R. Liao, D. Moyer, M. Cha, K. Quigley, S. Berkowitz, S. Horng, P. Golland, and W. M. Wells, “Multi-modal representation learning via maximization of local mutual information,” in *International Conference on Medical Image Computing and Computer-Assisted Intervention*. Springer, 2021, pp. 273–283.
- [57] M. Cooke, J. Barker, S. Cunningham, and X. Shao, “An audio-visual corpus for speech perception and automatic speech recognition (I),” *The Journal of the Acoustical Society of America*, vol. 120, pp. 2421–4, 12 2006.
- [58] J. Barker, R. Marxer, E. Vincent, and S. Watanabe, “The third ‘chime’ speech separation and recognition challenge: Analysis and outcomes,” *Computer Speech & Language*, vol. 46, 10 2016.
- [59] K. Yang, D. Markovic, S. Krenn, V. Agrawal, and A. Richard, “Audio-visual speech codecs: Rethinking audio-visual speech enhancement by re-synthesis,” in *Proceedings of the IEEE/CVF Conference on Computer Vision and Pattern Recognition (CVPR)*, 2022.
- [60] A. Adeel, M. Gogate, A. Hussain, and W. Whitmer, “Lip-reading driven deep learning approach for speech enhancement,” *IEEE Transactions on Emerging Topics in Computational Intelligence*, vol. PP, pp. 1–10, 09 2019.